전자기 과도현상 해석을 위한 주파수 의존 시스템 등가

論 文
56-9-5

Frequency Dependent Network Equivalent for Electromagnetic Transient Studies

王 龍 泌† · 曺 金 植*
(Yong-Peel Wang · Keum-Sik Jo)

Abstract - The complexity of modern power systems often makes it impractical to model it in its entirety for electromagnetic transient studies. Therefore areas outside the immediate area of interest must be represented by some form of Frequency Dependent Network Equivalent (FDNE). The advantage of using z-domain fitting is that it can be directly implemented in a digital simulation program without any loss of accuracy. Fitting in the s-domain always requires "discretizing" a continuous system and the inherent approximations. This paper presents z-domain rational function formulation and demonstrates the use of it for the assessment of the transient response of the Lower South Island of New Zealand. Moreover by using a well publicized test system and providing complete information on the developed FDNE coefficients other researchers easily benchmark their work against this.

Key Words : Electromagnetic Transient, Frequency Dependent Network Equivalents, AC System Representation

1. Introduction

Although time domain techniques, such as used in EMTP and PSCAD/EMTDC packages, can accurately perform analysis of power system transients, detailed representation of a large complex power system will entail a prohibitive amount of computation. Hence there is a need to have equivalents which adequately represent the areas outside the immediate area of interest. These are called Frequency Dependent Network Equivalents (FDNE) as the requirement to adequately represent the transient behaviour means it must mimic the frequency response of the system in represents. Therefore conventional equivalents based on the fundamental frequency short circuit level are inadequate for representing the external networks behaviour when simulating transients, due to the presence of other frequency components.

Early FDNEs modelled the external system by an appropriate network of lumped R, L and C components whose values are chosen so the equivalent network will have the same frequency response as the external network. Using RLC components allows implementation in existing transient programs with minimal change, however it restricts the possible frequency response that can be represented. The use of rational functions in s (or z) domain is more general and this has been the dominant approach in recent years. The fitting techniques used for modelling frequency-dependent effects in transmission lines are equally applicable to FDNEs. One of the motivations for investigating z-domain fitting is that it can be directly implemented in a digital simulation program without any loss of accuracy as it is already a discrete formulation. Fitting in the s-domain always requires "discretizing" a continuous system and has inherent approximations. The work of Hingorani & Burbury[1], Abur & Singh[2-3], Gustavsen & Semlyen[4], Angelidis & Semlyen[5], and Morched, Ottevangers & Marti[6] are particularly noteworthy. The use of z-domain FDNEs was reported in ref [7].

Although, as the order of the fitted model increases, the general tendency is for the accuracy of the fit to improve, at a certain point the algorithm will fit unstable poles, thereby making the model useless. Parameters such as the frequency range and weighting factors used for fitting, influence whether unstable poles are generated. Moreover a 3-phase FDNE can be unstable even if all the self and mutual terms are fitted by stable rational

† 교신저자, 正會員 : 東亞大 工大 電氣工學科 招聘教授 · 工博
E-mail : ypwang@daunet.donga.ac.kr
* 正 會 員 : 韓國電力公社 昌原電力管理處 系統運營副長
接受日字 : 2007年 6月 26日
最終完了 : 2007年 8月 17日

functions, if the 3 X 3 matrices are not positive definite at all frequencies. This problem has been tackled by Gustavsen & Semlyen[9] for s-domain fitting. Most work on FDNE has used s-domain rational function, or partial fraction form, whereas the present work uses a rational function in the z-domain. Ref [7] introduced the concept of z-domain FDNE and demonstrated its use on simple single-phase systems (both single and two-port). A recent contribution outlines the least squares fitting technique and applies it to a practical test system (Lower South Island of New Zealand)[8]. Although it used a full 3 X 3 representation (including mutual coupling), it is clear from the response that this FDNE is not optimal. The paper compared various FDNEs (including the use of RLC networks) for harmonic assessment on a test system which includes an HVDC link.

This paper demonstrates the accuracy achievable for transient analysis of a practical system by applying the enhanced FDNE to the Lower South Island of New Zealand. One of the objectives of this paper is to provide a benchmark for this type of work. The Lower South Island was an actual system and all the input data, such as line geometry, transformer parameters... etc, is available in published literature[10]. The inclusion of all the FDNE coefficients allows the transient response of this FDNE to be assessed easily and compared with those generated by other methods.

2. Derivation of Frequency Response

The development of a frequency dependent network equivalent (FDNE) requires knowledge of the frequency response of the system to be represented. The modelling of the frequency dependence of overhead lines and cables is well advanced in electromagnetic transient packages, but this is not the case with other system components; for instance the standard models of generators, transformers and loads do not represent the increase in resistance (and slight reduction in inductance) associated with skin effect. Therefore the use of a frequency domain program will give a frequency response closer to reality. However, if the FDNE is developed from the frequency response obtained from a frequency domain program its accuracy can only be assessed by corresponding measurements in the real system, which is not a practical proposition. Hence for verification purposes, the approach taken in this paper is the derivation of the frequency response from the less accurate time domain simulation, as this allows the complete time domain model to be used as the benchmark. The New Zealand Lower South Island shown in Fig. 1 is used as a test system with a resistive load connected to the Tiwai bus and fault is applied to phase C.

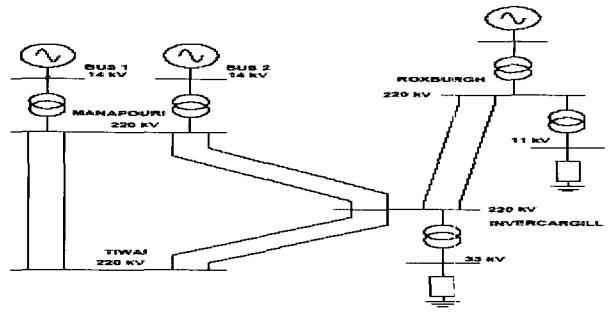

Fig. 1 Lower south island of New Zealand test system

Three tests are performed (injecting current in one phase at a time), with the fundamental frequency voltage sources removed, to derive the self and mutual impedances at each frequency. The resulting 3 X 3 impedance matrices are then inverted to provide the admittance matrices to be fitted. The off diagonal elements of this matrix, with negative sign, constitute the admittances of the interconnecting branches to be fitted, while the diagonal elements (which are the sum of all the branch admittances connected to the node) constitute the shunt terms (Y_{self}) to be fitted. As the admittance matrix is symmetrical (i.e. Y_{12} is equal to Y_{21} and Y_{13} is equal to Y_{31}) only six terms need to be fitted. Finally for the comparison the fitted terms are inverted to derive the impedances.

3. Structure Of The Frequency Dependent Network Equivalents

The three-phase system equivalent of the test system will be of the form shown in Fig. 2, where each frequency dependent block is represented by a rational function.

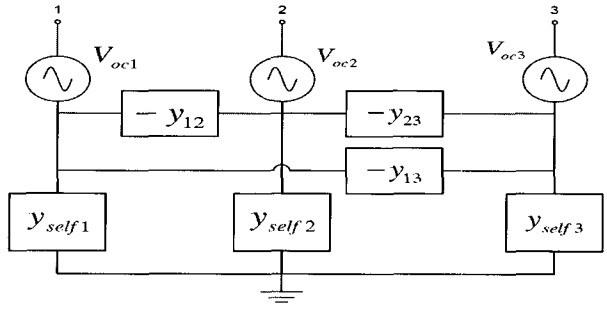

Fig. 2 Three-phase FDNE

2.1. Obtaining the Rational Function from Frequency Response

Each term is represented by a rational function of the form.

$$H(z)=\frac{a_0+a_1z^{-1}+a_2z^{-2}+\cdots+a_mz^{-m}}{b_0+b_1z^{-1}+b_2z^{-2}+\cdots+b_mz^{-m}} \quad (1)$$

Evaluating the frequency response of the rational function and equating it to the required values gives:

$$H(j\omega)=\frac{\sum_{k=0}^{m}(a_k z^{-kj\omega\Delta t})}{1+\sum_{k=1}^{m}(b_k z^{-kj\omega\Delta t})} \quad (2)$$

Adding weighting factors to reduce steady-state error yields:

$$H(j\omega)=-\sum_{k=1}^{m}((b_k\cdot H(j\omega)-a_k)\varepsilon^{-kj\omega\Delta t})+a_0 \quad (3)$$

Splitting into real and imaginary components (using $\varepsilon^{-kj\omega\Delta t}=\cos(k\omega\Delta t)-j\sin(k\omega\Delta t)$ gives:

$$-c(j\omega)=\sum_{k=1}^{m}(b_k\cdot(c(j\omega)\cos(k\omega\Delta t)+d(j\omega)\sin(k\omega\Delta t))-a_k\cos(k\omega\Delta t))-a_0 \quad (4)$$

$$-d(j\omega)=\sum_{k=1}^{m}(b_k\cdot(d(j\omega)\cos(k\omega\Delta t)-c(j\omega)\sin(k\omega\Delta t))-a_k\sin(k\omega\Delta t)) \quad (5)$$

The values of the a and b coefficients are determined by setting up an over-determined system of linear equations of the form:

$$\begin{bmatrix}A_{11} & A_{12}\\ A_{21} & A_{22}\end{bmatrix}\begin{bmatrix}\underline{a}\\ \underline{b}\end{bmatrix}=\begin{bmatrix}\underline{C}\\ \underline{D}\end{bmatrix} \quad (6)$$

where

$\underline{a}^T=[a_0,a_1,a_2,\cdots,a_m]$, $\underline{b}^T=[b_1,b_2,\cdots,b_m]$,

$\underline{C}^T=[-c(j\omega_1),-c(j\omega_2),\cdots,-c(j\omega_n)]$,

$\underline{D}^T=[-d(j\omega_1),-d(j\omega_2),\cdots,-d(j\omega_n)]$

$$A_{11}=\begin{bmatrix}-1 & -\cos(\omega_1\Delta t) & \cdots & -\cos(m\omega_1\Delta t)\\ -1 & -\cos(\omega_2\Delta t) & \cdots & -\cos(m\omega_2\Delta t)\\ \vdots & \vdots & \ddots & \vdots\\ -1 & -\cos(\omega_n\Delta t) & \cdots & -\cos(m\omega_n\Delta t)\end{bmatrix}$$

$$A_{21}=\begin{bmatrix}0 & \sin(\omega_1\Delta t) & \cdots & \sin(m\omega_1\Delta t)\\ 0 & \sin(\omega_2\Delta t) & \cdots & \sin(m\omega_2\Delta t)\\ \vdots & \vdots & \ddots & \vdots\\ 0 & \sin(\omega_n\Delta t) & \cdots & \sin(m\omega_n\Delta t)\end{bmatrix}$$

$$A_{12}=\begin{bmatrix}R_{11} & R_{12} & \cdots & R_{1m}\\ R_{21} & R_{22} & \cdots & R_{2m}\\ \vdots & \vdots & \ddots & \vdots\\ R_{n1} & R_{n2} & \cdots & R_{nm}\end{bmatrix}$$

$$A_{22}=\begin{bmatrix}S_{11} & S_{12} & \cdots & S_{1m}\\ S_{21} & S_{22} & \cdots & S_{2m}\\ \vdots & \vdots & \ddots & \vdots\\ S_{n1} & S_{n2} & \cdots & S_{nm}\end{bmatrix}$$

$R_{ik}=c(k\omega_i)\cos(k\omega_i\Delta t)+d(k\omega_i)\sin(k\omega_i\Delta t)$

$S_{ik}=d(k\omega_i)\cos(k\omega_i\Delta t)-c(k\omega_i)\sin(k\omega_i\Delta t)$

m = Oreder of fit.

n = Number if frequency sample point

2.1. Implementation in Time Domain

From eqn. (1)

$$I(z)=a_0V(z)+(a_1z^{-1}+a_2z^{-2}+\cdots+a_mz^{-m})V(z)+(b_1z^{-1}+b_2z^{-2}+\cdots b_mz^{-m})i(z)$$

$$= G_{equiv} + I_{History} \quad (7)$$

Hence in discrete time:

$$i(n\Delta t)=a_0v(n\Delta t)+a_1v(n\Delta t-\Delta t)+a_2v(n\Delta t-2\Delta t)+\cdots+a_mv(n\Delta t-m\Delta t)+b_1i(n\Delta t-\Delta t)+b_1v(n\Delta t-2\Delta t)+\cdots+b_mi(n\Delta t-m\Delta t) \quad (8)$$

$i(n\Delta t)=G_{equiv}\cdot v(n\Delta t)+I_{History}$

where $G_{equiv}=a_0$

$$I_{History}=a_1v(n\Delta t-\Delta t)+a_2v(n\Delta t-2\Delta t)+\cdots+a_2v(n\Delta t-m\Delta t)+b_1i(n\Delta t-\Delta t)+b_2i(n\Delta t-2\Delta t)+\cdots+b_mi(n\Delta t-m\Delta t)$$

In eqn. (6) C and D are vectors of the negative of the real and imaginary parts respectively, of the sample data at each frequency. The system of linear equations is derived by evaluating the frequency response of H(z) and equating to the required response at each sample point. This is solved via weighted least-squares. Two equations result from each sample point, one for the real component and the other for the imaginary component. A weighting factor of 100 is applied to equations representing the fundamental frequency so as to ensure minimal steady-state error.

The resistance represents the instantaneous term ($1/a_0$) while the current source represents all the past history terms in current (a_1, a_2 $\cdots$ a_n) and voltage (b_1, b_2 $\cdots$ b_n). The complete formulation and implementation for this approach is given in ref. [10].

The rational function forms a finely balanced system that represents the frequency response of the system. The positive and negative coefficients result in very similar numbers being subtracted and hence precision is important in the calculations. Thus a large number of decimal places is needed.

Rounding the coefficients to fewer significant digits can have a dramatic effect on the frequency response and often results in the system being unstable. Fig. 3 displays the typical fitting accuracy for the Y_{self1} term (7^{th} order). Although increasing the order of the Y_{self1} improves the fit, some poles are unstable. The least-squares approach always seems to give a better fit at the higher frequencies compared to the lower, hence weighting factors are required to counter this. The simplest is applying a weighting for the fundamental component, however, other frequency dependent weighting factors have been tried.

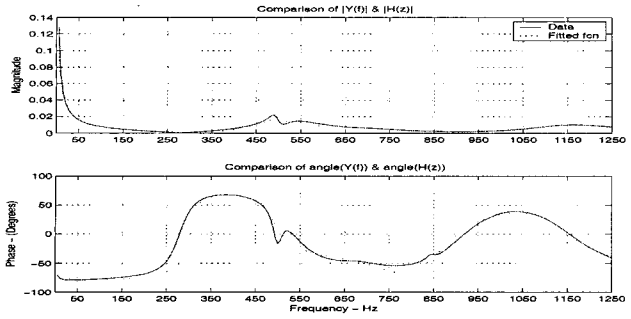

Fig. 3 Comparison of admittance Yself1 term

The voltage sources (magnitude and phase angle) for all the FDNEs are set to be that of the full system under open circuit. These values are given in Table 1.

Table 1 FDNE voltage source parameters

	Voltage(Phase a Neutral)	
	Magnitude (kV)	Phase Angle (deg.)
Phase A	121.599	61.16755
Phase B	121.599	-59.15545
Phase C	121.599	180.66100

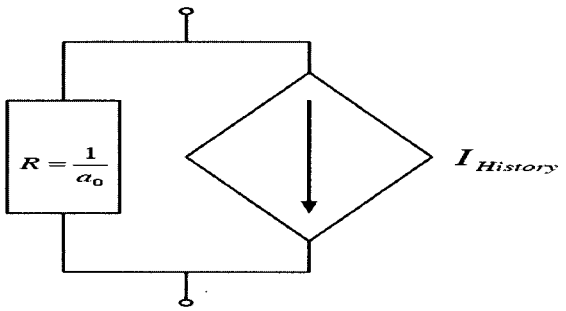

Fig. 4 Norton representation of a rational function

4. Simulations

The simulations performed using PSCAD/EMTDC, consist of a single-phase fault represented by a 0.001[Ω] resistance. applied to phase C at 0.815[s] and removed after 0.05[s]. The comparison of the Full system and FDNE (using a frequency range of 5-1250[Hz] for fitting) solutions is displayed in Fig. 5 and the coefficients used are given in [10]. The period immediately after fault inception (expanded in Fig. 7) is practically identical in both cases, while slight differences are noticeable after fault removal . The phase currents are shown in Figs. 8 -9.

Close inspection of these shows that the FDNE equivalent mimics the full system well; however, there is a low frequency component that causes a growing phase lag in the voltage during the fault period. This means that when the fault is removed there is a slight discrepancy in the voltage between the Full and FDNE solutions which accounts for the slight differences in the transient on fault removal. This phase difference vanishes within approximately 0.25[s] of fault removal.

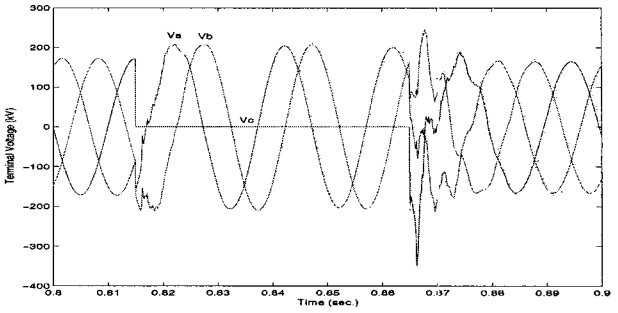

Fig. 5 Comparison of transient assessed using full system and FDNE representation, solid-full system, dotted-FDNE

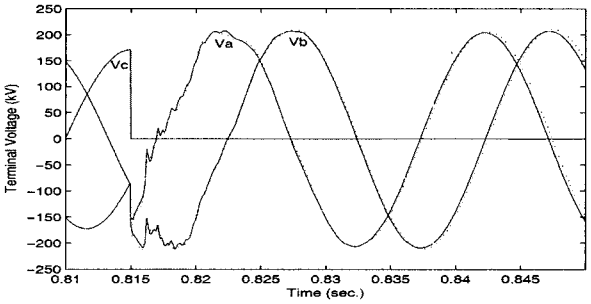

Fig. 6 Fault Inception, solid-full system, dotted-FDNE

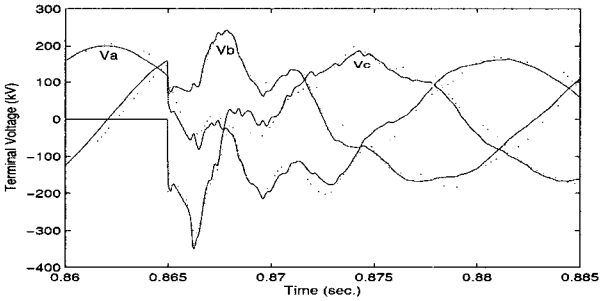

Fig. 7 Fault removal, solid-full system, dotted-FDNE

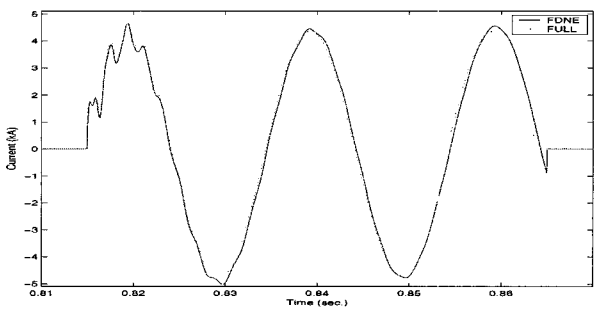

Fig. 8 Current in unfaulted phase (phase C), solid-full system, dotted-FDNE

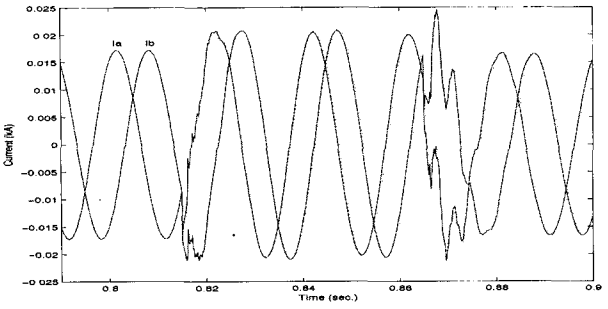

Fig. 9 Current in unfaulted phase (phase A and B), solid-full system, dotted-FDNE

To investigate the influence of the fitted frequency range on transient performance, FDNEs were also developed using the 5-2500[Hz] and 5-500[Hz] frequency ranges. Also, for comparison, a Thevenin equivalent (whereby each block in Fig. 2 is represented by an RL branch) based on the 50[Hz] admittance was simulated . The RL is implemented using the appropriate rational function where $a_0 = a_1 = \frac{1}{R+2L/\Delta t}$ and $b_1 = \frac{R-2L/\Delta t}{R+2L/\Delta t}$.

Table 2 shows the order of the rational function that was used for each term, for the various frequency ranges.

Table 2 Rational function order for various fitting frequency ranges

Term	Order		
	5-500	5-1250	5-2500
Y_{self1}	6	7	15
Y_{self2}	6	12	15
Y_{self3}	6	7	15
Y_{12}	8	11	17
Y_{13}	7	11	17
Y_{23}	8	11	17

Table 3 gives the R & L values used to model each of the admittance terms while Table 4 displays the coefficients used to implement this RL branch.

Table 3 Rational function order for various fitting frequency ranges

Term	Ohms	Henries
Y_{self1}	11.842	0.19647
Y_{self2}	11.879	0.20655
Y_{self3}	11.842	0.19647
Y_{12}	19.514	0.34898
Y_{13}	19.644	0.39479
Y_{23}	19.515	0.34899

In these comparisons the fault duration was not specified as removal occurs on the first current zero after 0.025[s] following fault application. Tables 5 to 10 give the coefficients used in PSCAD/EMTDC simulation for the 5-500[Hz] frequency range.

Table 4 Coefficients for rational function representing RL

Term	Order	
	a0(=a1)	b1
Y_{self1}	1.2705353612953927e-04	-9.9699092078614049e-01
Y_{self2}	1.2086071925372443e-04	-9.9712853546340041e-01
Y_{self3}	1.2705353612953927e-04	-9.9699092078614049e-01
Y_{12}	7.1537366252693527e-05	-9.9720809601966065e-01
Y_{13}	6.3246286117103626e-05	-9.9751517353535690e-01
Y_{23}	7.1534755297287628e-05	-9.9720806584012944e-01

Table 5 Coefficients for rational function representing Y_{self1} term

Order	a	b
0	3.0078294923663079e-03	1.0
1	-1.6867157879437031e-02	5.8699942174618052e+00
2	3.9394334773642417e-02	1.4405484110295935e+01
3	-4.9025038511999172e-02	-1.8918195083417309e+01
4	3.4265228069600508e-02	1.4022321525318672e+01
5	-1.2743659396358313e-02	-5.5620099984815141e+00
6	1.9684664251101679e-03	9.2239367111043769e-01

Table 6 Coefficients for rational function representing Y_{self2} term

Order	a	b
0	2.4466368842016076e-03	1.0
1	-1.3673558091512085e-02	-5.8774107818227614e+00
2	3.1809746270842362e-02	1.4441679174219205e+01
3	-3.9405381653974635e-02	-1.8988979106062335e+01
4	2.7395429619140748e-02	1.4091654909120685e+01
5	-1.0125536046686263e-02	-5.5960216493182253e+00
6	1.5526659700345685e-03	9.2907746088487098e-01

Table 7 Coefficients for rational function representing Y_{self3} term

Order	a	b
0	3.0078294923663079e-03	1.0
1	-1.6867157879437031e-02	-5.8699942174618052e+00
2	3.9394334773642417e-02	1.4405484110295935e+01
3	-4.9025038511999172e-02	-1.8918195083417309e+01
4	3.4265228069600508e-02	1.4022321525318672e+01
5	-1.2743659396358313e-02	-5.5620099984815141e+00
6	1.9684664251101679e-03	9.2239367111043769e-01

Table 8 Coefficients for rational function representing Y_{12} term

Order	a	b
0	6.6876629787707654e-03	1.0
1	-5.1491335355811199e-02	-7.1955469088034087e+00
2	1.7424585227718672e-01	2.2489101993989813e+01
3	-3.3855097683174190e-01	-3.9786978675039855e+01
4	4.1315377108245688e-01	4.3445034023350161e+01
5	-3.2433392314869508e-01	-2.9847753735867922e+01
6	1.5996468074640230e-01	1.2512802920585504e+01
7	-4.5324861745415362e-02	-2.8933709408255108e+00
8	5.6491299976239055e-03	2.7671132262133130e-01

Table 9 Coefficients for rational function representing Y_{13} term

Order	a	b
0	1.7399872694598111e-03	1.0
1	1.1263856073053968e-02	-6.7774986009704321e+00
2	3.1262831838239538e-02	1.9725734762103109e+01
3	-4.8223950008405743e-02	-3.1956619989073147e+01
4	4.4649362195819012e-02	3.1120004223321381e+01
5	-2.4814410002616423e-02	1.8215063623245992e+01
6	7.6656127060372083e-03	5.9329131941526958e+00
7	-1.0155778304361271e-03	-8.2946996474582613e-01

Table 10 Coefficients for rational function representing Y_{23} term

Order	a	b
0	6.6879759169563204e-03	1.0
1	-5.1491829884128787e-02	-7.1943188253680557e+00
2	1.7424233072110848e-01	2.2480775327153474e+01
3	-3.3853666697027623e-01	-3.9762719625266101e+01
4	4.1313051174614734e-01	4.3405670023731673e+01
5	-3.2431375927022815e-01	-2.9809336292797784e+01
6	1.5995509304323929e-01	1.2490254511167217e+01
7	-4.5322602381628350e-02	-2.8860022832352925e+00
8	5.6489470797505929e-03	2.7567716462752406e-01

Fig. 10 and 11 show an expanded view of the terminal voltage on fault application and removal. All, except the 50[Hz] based RL equivalent, give a good representation of the full system with the main error at fault removal due to the phase shift. Fig. 12 shows the same comparison for current (without the RL equivalent). Careful inspection of the current error, displayed in Fig. 13, shows that the greater the frequency range used for the fitting, the smaller the initial error; however, after 0.02[s] all equivalents, even the 50[Hz] based RL equivalent, give the same error. This error is due to the low frequency component causing the phase shift. Inspection of the error in the terminal voltage is very similar to the current error.

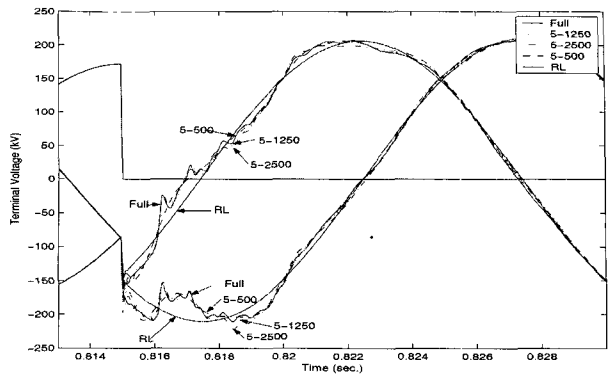

Fig. 10 Comparison of terminal voltage for fault application

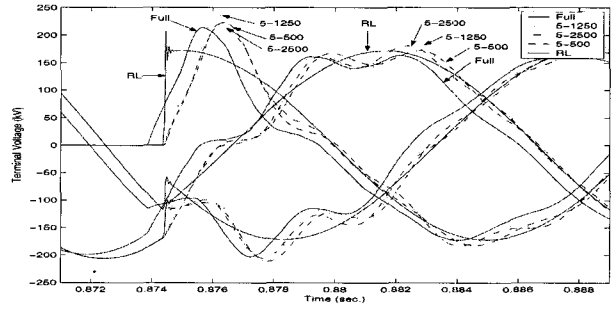

Fig. 11 Comparison of terminal voltage for fault removal

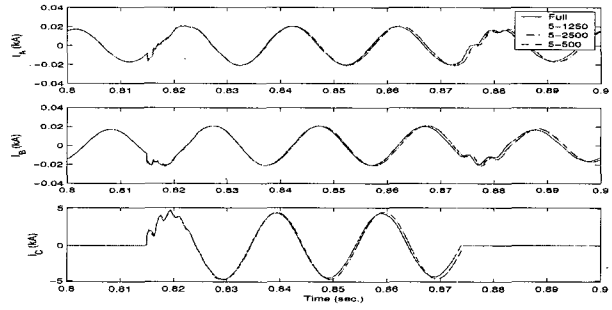

Fig. 12 Comparison of current waveforms

There are two stability issues, the stability of the individual rational functions and the stability of the set of rational functions. For instance, in the 5-2500[Hz[fitting range, Y_{12} can be fitted with a stable rational function of order 19, however, the resulting system of rational functions is unstable.

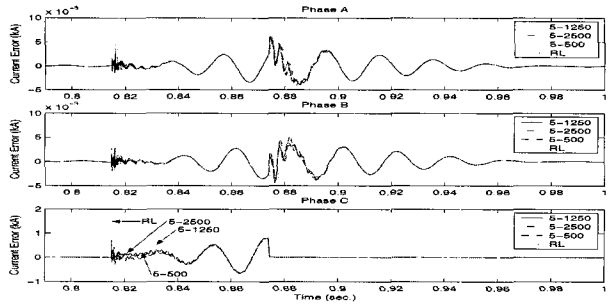

Fig. 13 Comparison of current error

5. Conclusion

The weighted least-squares fitting of a z-domain rational function has been formulated and its application to the development of a frequency dependent network equivalent of a practical system has been demonstrated. Full information of the derived FDNE has been given, allowing the transient response of this FDNE to be easily assessed and compared to other FDNEs developed for the same test system.

The effect of frequency range used to develop the FDNE has been shown and compared to an RL equivalent based on fundamental frequency information.. Although the frequency range determines the error in the first cycle after a disturbance, after this period the phase shift from a low frequency component dominates. All the equivalents give the same error after 0.04[s]. There is a need to improve the fit below 50[Hz] in order to remove this phase shift.

References

[1] N.G. Hingorani and M. Burbury, ''Simulation of ac system impedance in HVdc system studies'', IEEE Trans. on Power Apparatus and Systems, Vol. 89, No. 5/6, 1970, pp 820-828

[2] A. Abur and H. Singh, ''Time Domain Modeling of External Systems for Electromagnetic Transient Programs", IEEE Trans. on Power Systems, Vol. 8, No. 2, May 1993, pp 671-679

[3] H. Singh and A. Abur, ''Multi-Port equivalencing of External Systems for Simulation of Switching Transients", IEEE Trans. on Power Delivery, Vol. 10, No. 1, January 1995, pp 374-382

[4] B. Gustavsen and A. Semlyen, ''Rational Approximation of Frequency Domain Responses by Vector fitting", IEEE/PES Winter Meeting 1997}. Paper No. PE-194-PWRD-0-11-1997

[5] G. Angelidis and A. Semlyen, ''Direct Phase-Domain Calculation of Transmission Line Transients Using Two-Sided Recursions", IEEE Trans. on Power Delivery, Vol. 10, No. 2, April 1995, pp 941-947

[6] A.S. Morched , J.H. Ottevangers and L. Marti, "Multi Port Frequency Dependent Network Equivalents for the EMTP", IEEE Trans. on Power Delivery, Volume: 8 Issue: 3 , July 1993, pp 1402-1412

[7] N.R. Watson, A.M. Gole, and G.D. Irwin, ''Z-Domain Frequency-Dependent Network Equivalents for Electromagnetic Transient Studies", Proceedings of International Conference on Power System Transients (IPST'99), June 1999, pp 37-42

[8] Y.P Wang and N.R. Watson, "Z-Domain Frequency-Dependent A.C. System Equivalent for Electromagnetic Transient Simulation", IEE Proc. Genr. Transm. & Distrib., Vol. 150, No. 2, March 2003, pp 141-146

[9] B. Gustavsen and A. Semlyen, ''Enforcing passivity for admittance matrices approximated by rational functions", IEEE Trans. on Power Systems, Volume: 16 Issue: 1 , Feb 2001,pp 97 -104

[10] N.R. Watson and J. Arrillaga, "Frequency-Dependent A.C. System Equivalents for Harmonic Studies and Transient Convertor Simulation'', IEEE Trans. on Power Delivery, Vol.3, No. 3, July 1988, pp 1196-1203

[11] N.R. Watson and J. Arrillaga, Power Systems Electromagnetic Transients Simulation, IEE Books, U.K., 2002

저 자 소 개

왕 용 필 (王 龍 泌)

1966년 8월 25일생. 1992년 동아대 전기공학과 졸업. 1994년 동대학원 전기공학과 졸업(석사). 1998년 동대학원 전기공학과 졸업(공박), 1999년-2001년 뉴질랜드 Canterbury University (Post-Doc). 현재 동아대학교 전기공학과 초빙교수. 관심분야 : 직류송전 시스템 해석 및 제어설계, 전자기 과도현상, 전력품질(고조파, 플리커)

Tel : 051-200-6944

Fax : 051-200-7743

E-mail : ypwang@daunet.donga.ac.kr

조 금 식 (曺 金 植)

1954년 9월15일생. 1988년 부산개방대학교 전기공학과 졸업. 1993년 동아대학교 대학원 전기공학과 졸업(석사). 1975년-1978년 한국전력공사 부산화력발전소 1978년-현재 한국전력공사 창원전력관리처 계통운영부장. 관심분야 : 전자기 과도현상, 전력품질(고조파, 플리커)

Tel : 055-268-2330

Fax : 055-268-2329

E-mail : joksi@kepco.co.kr